Spectrally selective absorber coating of WAlN/WAlON/Al_2O_3 for solar thermal applications

Atasi Dan,[a] J. Jyothi,[b] Kamanio Chattopadhyay,[c] Harish C. Barshilia,[b, #]

Bikramjit Basu [a, c, #]

[a] Materials Research Centre, Indian Institute of Science, Bangalore-560 012, India
[b] Nanomaterials Research Laboratory, Surface Engineering Division, CSIR-National Aerospace Laboratories, HAL Airport Road, Kodihalli, Bangalore 560 017, India
[c] Materials Engineering and Interdisciplinary Centre for Energy Research, Indian Institute of Science, Bangalore-560 012, India

Abstract

A novel WAlN/WAlON/Al_2O_3 coating was successfully deposited on stainless steel (SS) substrate using reactive DC and RF magnetron sputtering. Excellent spectrally selective property with a high absorptance of 0.958 in the solar spectrum region and low emittance of 0.08 in the infrared region were achieved by tailoring the target power, deposition time and the reactive flow rates of N_2 and O_2. In the present solar selective coating, W layer acts as a back reflector and diffusion barrier, WAlN as the main absorber layer, WAlON as the semi-absorber layer, whereas the topmost Al_2O_3 layer works as an anti-reflecting layer. In reference to the thermal stability, the absorber deposited on SS substrates exhibited high solar selectivity (α/ε) of 0.920/0.11, when heat treated in air up to 500°C for 2 hours. Taken together, the present study demonstrated that the WAlN/WAlON/Al_2O_3-based selective absorbing coating with excellent thermal stability could be a promising material for photo-thermal conversion at temperatures of up to 500°C.

Keywords: Tungsten aluminium nitride, spectral selectivity, optical properties, thermal stability, sputtering

[#] Corresponding Authors:
Email: harish@nal.res.in (Harish C. Barshilia)
bikram@mrc.iisc.ernet (Bikramjit Basu)

1. Introduction:

Concentrating solar power (CSP) system is one of the technologically emerging approaches, which can be implemented to convert the enormous amount of solar energy to usable form of energy, like electricity or heat [1, 2]. The efficiency of these systems strongly depends on the solar selective absorber coating deposited on the metallic receiver tube. An ideal solar selective absorber coating should exhibit a high absorptance ($\alpha \geq 0.95$) in the wavelength range of 0.3–2.5 μm and a low emittance (≤ 0.10) in the infrared region ($2.5 \leq \lambda \leq 25$ μm) [3, 4]. In addition, a solar selective absorber coating should have excellent thermal stability at high temperature ($\geq$ 400°C) [5]. A number of techniques such as, electrodeposition, physical vapour deposition, chemical vapour deposition, sol-gel, paint technology, etc. have been used to fabricate the solar selective coatings [6-10]. To address the high temperature stability of the coatings, environment friendly magnetron sputtering technology with various advantages, like large area deposition, high deposition rates, reproducibility, precise control in thickness and deposition parameters, etc. has become popular to develop these coatings in last several decades [10].

To achieve superior spectral selectivity and high temperature stability, a variety of solar selective coatings, such as single-layer cermet coatings, absorber-reflector tandem, semiconductor coatings, metal-dielectric composite coatings etc. have been studied and reported elsewhere [11, 12]. One important reason limiting the use of the single layer cermet coatings is that their optical property degrades quickly at high temperature due to change in their microstructure and oxidation. In order to ensure the persistency of the coating at elevated temperature, one of the promising structures is the tandem absorber with graded metal concentration profile. Such designed structure consists of an anti-reflection surface layer of a transparent ceramic material, two solar absorptive intermediate layers and an IR-reflective metallic layer deposited on a metallic substrate [13].

Recently, transition metal nitrides and oxynitrides -based coatings have become popular as solar selective absorber due to their chemical inertness, outstanding spectral selectivity, superior chemical, mechanical, thermal stability and excellent oxidation resistance [14-16] . In particular, the tandem absorber coatings have been extensively investigated by a number of groups. For example, Ouyang et al. reported that TiAlN/TiAlSiN/Si_3N_4 coatings, deposited on SS substrates can exhibit high absorptance of 0.938 and thermal emittance of 0.09 [17]. According to Wang et al., NbTiON/SiON absorber coating, prepared on Cu substrate showed high selectivity with an absorptance value of 0.95 and emittance value of 0.07 [18]. Barshilia et al. studied TiAlN/TiAlON/Si_3N_4 and NbAlN/NbAlON/Si_3N_4 and these tandem absorbers showed high absorptance of 0.958 and 0.956, respectively and low emittance of 0.07 for both the coatings [19, 20]. In a different work, Wang et al. reported that high absorptance of 0.948 and low emittance of 0.05 could be achieved by multilayerd coating of Al/NbMoN/NbMoON/SiO_2 on SS substrates [21]. In another study, Zou et al. reported a CrAlN–CrAlON based tandem absorber that exhibited a high absorptance of 0.984 and a low emittance of 0.07 [22]. These studies suggest that if a coating is fabricated, while replacing the transition metal with tungsten, the desired spectral selectivity can be obtained.

In the present W/WAlN/WAlON/Al_2O_3 coating, WAlN acts as the main absorber layer, WAlON acts as the semi absorber layer and Al_2O_3 works as the anti-reflection layer. The metallic content of the absorber layers decreased from substrate to surface and such gradation enables to change the property of the layers from metallic to dielectric. The structure of the absorber coating has been presented in Fig. 1.

The structural, chemical, and optical properties of WAlN/WAlON/Al_2O_3-based tandem absorber coatings have been investigated using X-ray diffraction (XRD), X-ray photoelectron spectroscopy (XPS), atomic force microscopy (AFM), micro-Raman

spectroscopy, solar spectrum reflectometer and emissometer, UV-Vis-NIR spectrophotometer and Fourier transform infrared spectroscopy (FTIR). The optical properties of the coatings have been investigated in air in the range of 350-550°C.

2. Experimental:

2.1. Coating deposition:

W/WAlN/WAlON/Al_2O_3 spectrally selective coatings were developed on stainless steel (35 mm × 35 mm × 2 mm) by reactive DC/RF magnetron sputtering using high purity (> 99.9%) W, Al and Al_2O_3 target, respectively at constant target current, substrate bias and substrate temperature. A pulsed DC power supply was used to deposit W, WAlN and WAlON layers and a RF generator was used to deposit the Al_2O_3 layer. Before being put in the vacuum chamber, the substrates were polished and were degreased by sonication in acetone and isopropyl alcohol. The dried substrates were mounted on a rotatable substrate holder inside the vacuum chamber. W, Al and Al_2O_3 targets have a diameter of 150 mm and thickness of 8 mm. A base pressure of 8.5×10^{-6} mbar was created inside the sputtering chamber, which was equipped with a turbomolecular pump. Prior to the deposition, the targets were cleaned by sputtering for 10 min with a bias voltage of -800 V in pure Ar atmosphere. The distance between substrate and sputtering target was 10 cm. The sputtering gas, Ar with a purity of 99.99% and the reactive gases, O_2 and N_2, with a purity of 99.99% were injected to the sputtering chamber separately and adjusted by standard mass flow controllers. The chamber pressure was controlled by a manual valve mounted between the chamber and pump to get the desired pressure. The W interlayer was deposited in Ar-plasma by the non-reactive sputtering of W target with a power density of 3.114 W/cm^2. The WAlN, WAlON and Al_2O_3 layers were prepared from the reactive sputtering of W, Al and Al_2O_3 targets in Ar + N_2, Ar + N_2 + O_2 and Ar + O_2 plasma, respectively. The Ar gas flow was kept constant at 28 sccm, while depositing W, WAlN and WAlON layers. The nitrogen flow rate

was 26 and 21 sccm for WAlN and WAlON layers, respectively while the O_2 gas flow rate for WAlON layer was 9 sccm. For the deposition of WAlN layer, the power densities of W and Al targets were 1.698 and 2.265, respectively. Sputtering of WAlON layer was carried out at a power density of 1.982 and 2.548 W/cm^2 for W and Al, respectively. The top Al_2O_3 layer was deposited at a power density 6.582 W/cm^2 of Al_2O_3 target in Ar and O_2 gas flow rate of 20 and 2 sccm, respectively. The time of deposition for W, WAlN, WAlON and Al_2O_3 layers are 15, 6, 6 and 6.5 min, respectively. The sputtering parameters for an optimized coating are summarized in the Table 1. Also, the effect of the deposition time on the selective property of the coating has been presented in Table 2.

2.2. Coating characterization:

The phase assemblage of the film was investigated by X-Ray Diffractometer (Bruker, D8) with Cu-K_α (40 kV, 40 mA, λ = 0.15406 nm) radiation in the 2θ range of 10° to 60°. The chemical composition and bonding structure of the coatings, deposited on Si substrates were probed by X-ray photoelectron spectroscopy (SPECS), using non-monochromatic Al K_α radiation (1486.8 eV). The binding energies reported here were calculated with reference to C 1s peak at 284.5 eV with a precision of 0.1 eV. Surface topography of the sample was studied using atomic force microscopy (AFM, Bruker) with a silicon nitride tip of radius 50 nm in contact mode. A DILOR-JOBIN-YVON-SPEX integrated micro-Raman spectrometer (Model Labram) was used to obtain the Raman spectra.

The total hemispherical absorptance and emittance of the tandem absorber were measured using solar spectrum reflectometer and emissometer (M/s. Devices and Services). The reflectometer and emissometer were calibrated with standard samples. The absorptance was measured at room temperature, whereas, for the emittance measurements, the emissometer detector was heated to 82°C. The accuracies of the measured absorptance values are ±2% and the emissometer has a repeatability of ±0.01 units. The absorptance and the

emittance values were measured at four different positions and the values reported here are the averages of four measurements. The reflectance spectra of the samples at 0° angle of incidence in the wavelength range of 0.3–2.5 μm were measured using UV–Vis–NIR spectrometer (PerkinElmer, Lambda 950), equipped with an integrating sphere. FTIR spectrometer (PerkinElmer) was used to record the reflectance spectra of the sample in the operating range of 2.5-25 μm.

In order to investigate the thermal stability, the tandem absorber coatings deposited on stainless steel substrates were kept inside a resistive tube furnace (Carbolite) in the temperature range of 300 – 550 °C for 2 hours in air. Annealing involved a step size of 50 °C with a heating rate of 10 °C/min.

3. Results:

The spectral property of a coating is strongly influenced by the deposition parameters [14]. Therefore, the power densities of the targets, the gas flow rates (O_2/ N_2) and the deposition time were tailored to achieve maximum absorptance in the solar spectrum region and minimum emittance in the infrared region. In the preceding section, the specific details of the deposition parameters are provided.

3.1.Structural properties:

3.1.1. Phase assemblage of the coatings:

X-ray diffraction patterns of WAlN, WAlON and Al_2O_3 layers, deposited on SS substrates are presented in Fig. 2. Each layer was deposited individually on stainless steel substrate for longer duration, keeping other deposition parameters, mentioned in Table 1 constant. The WAlN layer exhibited a strongest peak at a d-spacing of 2.520 Å, corresponding to crystallographic plane (111) of cubic AlN. The XRD pattern of WAlN reveals that the deposited thin film is nano-crystalline in nature. The peak observed in the WAlON layer at d-spacing of 3.710 Å, can be assigned to (100) plane of cubic WO_3. This

broad peak indicates the formation of nano-crystalline WO_3. The peaks (*), obtained in the XRD pattern of Al_2O_3 layer, resemble very closely those of SS substrate. The resemblance of peak confirms the amorphous nature of Al_2O_3. This is attributed to the fact that the crystallization temperature of aluminium oxide is very high (1200°C) [23].

3.1.2. X-ray photoelectron spectroscopy:

To investigate the bonding states of the elements in the tandem absorber coatings using XPS, single layer of WAlN, WAlON and Al_2O_3 was deposited on silicon substrates under the same processing condition, as described in Table 1. A longer time of deposition was performed. Fig. 3 shows the core-level XPS from a coating of WAlN. The peaks at 32.7 and 34.7 eV in Fig. 3(a), originated from W $4f_{7/2}$ and W $4f_{5/2}$ electrons in WN and W_2N, respectively [24]. In addition, the peaks centred at 36.2 and 38.4 eV reveal the binding energies of W $4f_{7/2}$ and W $4f_{5/2}$ electrons in WO_3 phase [25]. The deconvolution of Al 2p spectrum in Fig. 3(b) resulted in four peaks centered at 72.9, 73.5, 74.5 and 75.2 eV. The peaks centered at 72.9 and 73.5 eV correspond to metallic Al and Al bound to nitrogen, respectively [26, 27]. The latter two components belong to Al attached to oxygen and oxynitride, respectively [28, 29]. N1s spectrum, shown in Fig. 3(c), reveals the presence of five peaks centered at 396.3, 396.7, 397.7, 398.6 and 400.1 eV. The peak at 396.3 eV can be attributed to nitrogen in nano-crystalline AlN [30]. The peak position, located at 396.7 and 397.7 eV, indicates the formation of WN and W_2N phases, respectively [31]. The peak, observed at 398.6 eV, can be assigned to the nitrogen attached with Al and O in N-Al-O bond [32]. The existence of N 1s electron in interstitial site of W_2N is revealed by a low intensity and broad peak at 400.1 eV [33]. The deconvulation of oxygen spectrum in Fig. 3d shows four peaks, centred at 530.5, 531.5, 532.8 and 532.9 eV. The peak at 530.5 eV corresponds to the O 1s peak of WO_3 [34]. The peak at 531.5 eV represents the O 1s electron in Al_2O_3 [35]. The low intensity peak at 532.8 eV is observed due to the chemisorption of water at the active

site of thin film surface [36]. The peak at 532.9 eV arises due to the formation of other combination states of WO_x [37]. A similar analysis of the core level spectra of WAlON and Al_2O_3 layers have been provided in the supplementary document (Fig. S1 and Fig. S2). The assignment of peaks for all these layers (WAlN, WAlON and Al_2O_3) have been summarized in Table 3.

3.2. Optical properties:

A selective coating should exhibit optical selectivity, i.e., the variation of optical properties from one spectral region to another. In case of a solar selective coating, the selectivity depends on the fraction of solar energy absorbed by the coatings in visible and the near- IR region and the thermal heat loss from the coating in the mid- and far- IR regions. Therefore, the absorptance and emittance are the two most important parameters to evaluate the efficiency of the coating. The absorptance and emittance values for SS substrate, SS/W, SS/W/WAlN, SS/W/WAlN/WAlON, and SS/W/WAlN/WAlON/Al_2O_3 are given in Table 4. It can be observed that the absoptance values of stainless steel substrate is 0.387. The absorptance reaches the value of 0.50 after deposition of W. The largest contribution in absorptance is from WAlN layer, which improves the absorptance to 0.753. The absorptance is further increased to 0.902 after incorporation of WAlON as a semi-absorber layer on top of WAlN layer. Finally, after deposition of Al_2O_3 as an anti-reflection layer, WAlN/WAlON/Al_2O_3 based tandem absorber coating exhibits a high absorptance of 0.958.). It is worthwhile to mention that the optical properties are very sensitive to any changes in the thickness of a coating. Therefore, a number of experiments have been performed systematically during optimization of the coating to understand the influence of the thickness on optical properties of W/WAlN/WAlON/Al_2O_3 coating. As the increase in deposition time leads to an increase in thickness, the successive layers were deposited on stainless steel substrates by varying the deposition time without changing any other deposition conditions of

Table 1. Table 2 shows the variations of the absorptance values of the layers with respect to deposition time. It can be observed that as we increase the deposition time, initially the absorptance increases for all the layers. After a certain point, further increase in deposition time results the decrease in absorptance. However, though the deposition has been performed for different times, the emittance of all the coatings were constant at 0.08 for the coatings studied in the present work.

It is well known in literature that the sunlight is absorbed due to destructive interference at the interface of the layers in the multilayer stack of the coating [38]. Therefore, the optical characteristics of the individual layer have also been evaluated by measuring the reflectance spectra of the individual layer in UV-Vis-NIR spectrophotometer in the solar spectrum range of 300-2500 nm and are presented in Fig. 4(a). As indicated by Fig. 4(a), the well-defined interference minima can be identified in each layer, except for stainless steel substrate. In W coated SS, one interference minimum is observed at 465 nm with 57% reflectance, whereas the minimum in SS/W/WAlN layer, located at 1258 nm with 20% reflectance. Thereafter, the reflectance increases with an increase in the wavelength. The reflectance spectra of WAlON undergoes significant change as two interference minima appears at 360 nm and 1293 nm. The values of reflectance in these two minima are reduced to 2% and 9%, respectively. The Al_2O_3 layer plays an important role in diminishing the reflectance by destructive interference. It yields a sharp interference minimum at 356 nm and another wider minimum covering wavelength of 870 to 1345 nm. The interesting phenomenon for WAlN/WAlON/Al_2O_3 layer is in the broad second interference minima. The reflectance of the interference maxima drops from 16% to almost 0%, when the wavelength increases from 491 nm to 870 nm and it remains at 0% up to 1345 nm. This induces a high absorptance in the solar spectrum region. The reflectance increases with increasing wavelength at $\lambda > 1500$ nm for all the layers and is higher than 50% at $\lambda > 2230$ nm. It can also be observed that, the first minima for each

successive layer shifts to higher wavelength side. Hence, the reflectance spectra of each layer, as shown in Fig. 5(a), are in good agreement with the results obtained from the solar reflectometer (Table 4).

For high temperature applications, the energy loss in the form of thermal emission has a significant impact in overall system efficiency. According to Stephan-Bolzman law, the thermal radiation loss of absorber is proportional to the fourth power of temperature [39]. Therefore, the evaluation of the thermal heat loss was carried out by measuring the emittance using a commercial emissometer, operating at 82°C. The desired emittance value should be as less as possible. The emittance value of a polished SS substrate is 0.12. The deposition of tungsten interlayer on stainless steel substrate significantly reduced the thermal radiative losses, i.e., emittance from 0.12 to 0.08. The emittance value is 0.08 after deposition of WAlN, WAlON and Al_2O_3 layers. In order to verify the thermal radiative property, the reflectance spectra of each layer was collected using FTIR spectrophotometer in the wide wavelength range from 2.5 to 25 μm. Fig. 4(b) illustrates that the reflectivity of the coating is > 90% in the most important range for thermal radiation, i.e., 3-25 μm.

The thermal stability is a critical point of concern for a solar selective absorber coating as these coatings need to be thermally efficient at high operating temperature. To investigate the thermal stability of the coatings, the samples were heated in air at the temperature range of 300°C to 550°C with holding at each temperature for 2 hours and subsequently the absorbers were allowed to cool at room temperature. The variation of absorptance and emittance as a function of temperature has been presented in Fig. 5(a). The recorded results indicate that the coating exhibits excellent thermal stability up to 500°C without any significant change in the selectivity. However, at 550°C, the absorptance decreases to 0.80-0.82 and the emittance substantially increases to 0.50. Such a change reflects a variation in selectivity of heat treated sample with respect to the as-deposited

sample. The high temperature performance of the spectrally selective coating is also evident from the corresponding reflectance spectra, as shown in Fig. 5(b). It represents the reflectance spectra of the as-deposited and thermally annealed coatings as a function of temperature in the temperature range of 300-550 °C. It can be noticed that there is almost negligible amount of increase in the reflectance up to 500 °C. Therefore, it can be stated that the absorptance of the coating is excellent up to 500 °C, which is a critical feature of the coating for its application in CSP systems. The sudden change in the reflectance spectra has been observed in the heat treated sample at 550 °C.

The microstructural stability of the tandem absorber at higher operating temperatures was investigated using micro-Raman spectroscopy. The Raman spectra of the as-deposited tandem absorber and tandem absorbers heat-treated at 450 and 550 °C are shown in Fig. 6. The spectrum of the as-deposited tandem absorber shows two featureless broad bands. There was no significant change in the Raman spectrum even after heating the sample up to a temperature of 450 °C, which indicates the stable microstructure of the tandem absorber. However, after heat treatment up to 550 °C, some peaks appear in the Raman spectrum. The peaks in the lower frequency range of 200 cm^{-1} corresponds to lattice vibration. The intense peaks centered at 215 and 280 cm^{-1} can be attributed to O-W and O-W-O bending mode [40, 41], respectively. It has been reported in the literature the Raman bands located in the range 600 - 950 cm^{-1} correspond to either the antisymmetric stretch of W-O-W bonds or the symmetric stretch of (-O-W-O-) bonds [42]. The peaks observed at 400, 489 and 525 cm^{-1} represents the vibrations of Fe-O functional groups in α-Fe_2O_3 [43, 44]. From the analysis of the Raman spectroscopy of the heat treated coating at 550 °C, it can be predicted that the heat treatment has introduced several modifications in the coating. Firstly, the W in the coating reacts with oxygen and formed WO_3, which agrees fairly well with the reported XRD result on the thermal stability of the present tandem absorber [45]. Secondly, the

difference in the thermal expansion co-efficient of the coating and the substrate results delamination of the multilayer stack. Therefore, a large amount of Fe diffusion from the surface becomes dominant to form a surface layer of α-Fe_2O_3. An appreciable amount of these contaminants are believed to be responsible for the degradation of the coating at higher operating temperatures.

As the long-term thermal stability of the coating is concerned, we have performed the heat treatment of the coating for pro-longed duration and the coating was thermally stable without significant degradation in selective property up to 350 °C and 450 °C for 550 and 150 hrs respectively. We have reported these results in our recent publications [45, 46].

3.3. Physical properties:

The cross-sectional FESEM micrograph in Fig. 7 of the tandem absorber indicated that the thickness of the absorber is ~ 160 nm. Fig. 8(a - c) show three dimensional AFM topographic images of as-deposited WAlN/WAlON/Al_2O_3 and heat treated coating at 450 and 550 °C in air for 2 hrs. The AFM images were taken over an area of 10 × 10 μm^2. The RMS roughness value for as deposited coating was 3 nm. The AFM image shows the uniform surface morphology of the coating. After heat treatment of the coating, the RMS roughness is increased slightly to 5 nm. At 550 °C, the RMS roughness of the coating reaches to 58 nm. The drastic change in the surface roughness increases the emissivity and causes the delamination of the coating at 550 °C.

4. Discussion:

The overall goal of our work was to fabricate WAlN/WAlON/Al_2O_3-based solar selective absorber coating to absorb solar radiation as much as possible keeping the thermal emittance minimum. In addition, the tremendous challenge of the coating is to withstand at higher operating temperatures [47]. Moreover, the coating should possess improved oxidation resistance and chemical inertness.

A specific strategy has been followed while designing the presently investigated tandem structure. It is well known that a wide variety of substrates including copper, aluminium and other metals could be used for solar selective applications [48] . But the low cost stainless steel substrate has attracted more interest as it has high melting point, high thermal conductivity, excellent corrosion resistance and outstanding infrared reflectance. The W layer has been deposited on stainless steel substrate as a diffusion barrier as it possess high melting point (3422°C). This can also reduce the emittance of the absorber coating due to its excellent infrared reflectance [49]. In the case of WAlN and WAlON layers, the incorporation of Al and O in tungsten nitride matrix causes the change in the "*d*" orbital electron density of W metal leading to a change in bonding structure. The change in the "*d*" orbital electron density not only results in the formation of possible compounds, but also it allows the changes in optical and electrical properties of layers. This phenomenon is expected to result in the high absoprtance in the solar spectrum and low emittance in the IR range. It is known that AlN possesses high thermal conductivity (180 W/mK at 25°C), good dielectric properties (dielectric constant = 8.8 at 1 MHz), good optical properties (i.e., wide band gap {6.2 eV}), refractive index (1.9–2.1), high decomposition temperature (2490°C), and chemical stability (in air up to 700 °C) [50]. Moreover, WN can act as a promising diffusion barrier as well as an adhesion promoter of underlying tungsten layer because of the refractory nature with excellent thermal, chemical and mechanical properties [33]. Al_2O_3, most widely used material in the ceramics family, exhibits superior anti-reflection property. That makes Al_2O_3 the choice for a wide range of optical applications [51]. It is expected that the combined properties of aluminium nitride, tungsten nitride and alumina will satisfy the requirement of desired optical properties and high temperature stability of the coatings.

The experimental results, described in the preceding section, demonstrate that the selective coating has been successfully deposited by controlling the various sputtering deposition conditions and it fulfils all conditions to be a promising spectrally selective absorber coating. The important point in this study is to understand the mechanism of selectivity in WAlN/WAlON/Al_2O_3 –based coating.

Again, let us consider the reflectance spectra of Fig. 4(a). It has been described that an increase in number of layers in the absorber coating reduces the reflectance and results in a shift of the interference minima towards higher wavelengths. These changes can be explained by a number of reasons. Previous studies suggest that the significant reduction of reflectance, i.e., efficient absorption of the solar radiation can be rationalised by intrinsic absorption as well as absorption due to interference. The latter mechanism plays a major role in this multilayer solar selective absorber coating [38]. A common thread in number of experimental and theoretical studies is to describe the major requirements of selectivity in terms of composition of each layer, number of layers, layer thickness and metallic gradation from bottom to top layer [52-56]. It is well known that achieving maximum absorptance with a single layer is very difficult. However, by increasing the number of layers and gradually changing from metallic to dielectric status, one can significantly reduce the reflectance of the absorbing layer in solar spectrum region. Such kind of coatings have been extensively reported. For example, Rebouta et al. achieved an absorptance of 0.96 and an emittance of 0.05 in a tandem absorber consisting of TiAlSiN/TiAlSiON/SiO_2 [57]. Wu et al. reported CrN_xO_y/SiO_2 solar selective absorber coating, which exhibited high absorptance of 0.947 and low emittance of 0.05 [48]. Barshilia et al. developed TiAlN/AlON tandem absorber with an absorptance of 0.931-0.942 and emittanc of 0.05-0.06 [58]. These multilayer coatings consist of ceramic top layers and metallic bottom layers with gradient layers in between. A graded metallic profile is characteristics of such

multi-layers and accounts for their selective absorbing capability of solar radiation [59]. A number of theoretical studies on solar selective absorber coating have led to the conclusion that the optical properties of these multilayer coating should be maintained in such a way that the bottom layer absorbs maximum sunlight, while top layer reduces the reflection from the front and the middle layer links the base and top layer [60-62]. Different physical models have been used to design and optimize the structure as well as the composition of the coating. The optimisation studies using these physical models showed that the highest photothermal efficiency was achieved by graded metallic feature, i.e., decreasing metal content towards the front surface of the stack. It should be mentioned that the correlation between the optical/electrical properties with the refractive index was used to optimize the selective property. These studies suggest that refractive index of each layer increases gradually with the increase in the metallic content of the layers. However, the effect of metal content and refractive index on the optical property of the WAlN/WAlON/Al_2O_3 –based coating can be illustrated in the same way as explained in the previous studies. Due to excellent nitriding resistance of tungsten metal, WAlN layer possesses metallic behaviour [61]. In another study, Zhao et al. reported that higher oxygen content in the Ni/NiO coating leads to lower electrical conductance i.e. lower metallic property [62]. This indicates that WAlON layer has lower metallic content than WAlN layer. On the other hand, Al_2O_3 is a pure dielectric and it has zero electrical conductance. Therefore, it should be pointed out that the requirement of gradient metal content has been satisfied in WAlN/WAlON/Al_2O_3 –based absorber coating.

In the present study, the shifting of the reflectance minimum in Fig. 4(a) towards higher wavelength clearly indicates the decrease of the metallic property, i.e., increase of the dielectric property from base layer to top layer of the coating. Such architecture results in the gradient refractive index of the multi-layer coatings. Therefore, metallic WAlN layer,

having high refractive index, works as a main absorber layer; The top dielectric Al_2O_3 layer with the lowest refractive index (n = 1.65) is used as anti-reflection layer [10], while the middle layer (WAlON) links the base and the top layer by reducing the reflectance with a material of intermediate refractive index. Furthermore, the thickness of the absorber coating has a strong effect on the optical properties of the coating. It may be noted that the individual layer thicknesses of the tandem absorber of the present work were ≈ 87, 50, 23 nm, respectively for WAlN, WAlON and Al_2O_3 layers with a total thickness of ≈ 160 nm (Fig. 7). Bostrom et al. studied the effect of the thickness on the reflectance property of solution-chemical derived Ni-Al_2O_3 coating [63]. They have shown that an increase in thickness of the coating also results in the shift of reflectance minima towards longer wavelength, i.e., the increase in absorptance. Hence, it can be confirmed from the reflectance spectra of successive layers that an increase in thickness of the absorber layer leads to an improvement of the optical properties of the WAlN/WAlON/Al_2O_3 coatings (see Fig. 4a).

While a high absorptance increases the efficiency of solar thermal conversion, it is equally important to reduce the emittance of the selective absorber to achieve highest possible photothermal conversion efficiency. The emittance values of the successive layers suggests that the careful optimization has been performed to control the emittance value along with high absorptance (Table 4). As discussed in the previous section, the emittance of the tandem absorber was controlled suitably by the incorporation of W interlayer.

However, one serious problem occurs when the coatings are exposed to high temperature due to change in their microstructure, component aggregation, diffusion and oxidation. Therefore, thermal stability of the solar absorber is one of the critical performance parameter because the absorber would degrade with time at the actual

application environment, which reduces the life time and eventually leads to failure. To improve the performance, one usual way is to deposit a thermally stable infrared reflecting metallic layer on stainless steel substrate. Not only the metallic layer holds on the good selective performance of the absorber coating at high temperature, but also it reduces the emissivity of the entire stack by minimizing the thermal radiative losses. In a recent work, Sibin et al. deposited W layer on stainless steel substrate to achieve low thermal emittance of AlTiN/AlTiON/AlTiO coating. This coating possessed a high absorptance of 0.955 and low thermal emittance of 0.08 with thermal stability up to 300 °C in air. Our focus to explore the selective property of W/WAlN/WAlON/Al_2O_3 –based solar selective coating was preliminary inspired by the work of Sibin et al [49]. It is worthwhile to mention that the advantage of presently investigated novel coating is the ease of scaling up the process as it needs only two targets (W and Al) to prepare the entire coating. The use of the oxide and oxynitride of W and Al has the advantages not only in logistic terms as the deposition process allows the use of less number of targets, but also these metals yield some exceptional properties, relevant for solar energy applications. Several reasons can be attributed to explain the high temperature stability of the present coating up to 500°C. It is well known that the optical properties of thin films depend on their method of preparation. The uniform composition and superior adhesion of the coatings make sputtering technique attractive compare to other processing techniques, like wet chemistry route, electro deposition and vapour deposition. Moreover, the high temperature stability of the coating has been achieved due to high thermal and structural stabilities for both the individual and combined layers, excellent adhesion between the substrate and adjacent layers and enhanced resistance to thermal and mechanical stresses [64]. The entire coating stack was structured by a pure metallic W layer at the substrate-absorber coating interface and Al_2O_3 as antireflection layer on the outside. Both the W

layer and Al_2O_3 layer serve as effective diffusion barriers. The W layer efficiently restrains the diffusion of iron and chromium from SS substrate to the absorber and restricts the occurrence of complex phases, which could be responsible for decreasing the absorptance and increasing the emissivity [65]. While aiming at reaching superior selective performance, we believed that Al_2O_3 is appropriate as an antireflection layer due to high thermal stability, chemical inertness and high melting point. The thermally stable Al_2O_3 layer prevents the diffusion of oxygen and other contaminants from the surrounding atmosphere towards the coating and provides the multilayer stack high temperature stability. Most importantly, the nano-composite and amorphous nature of the layers without grain boundaries provide added stability towards oxidation of metallic interlayer [66].

However, the annealed sample at 550°C, showed an unusual characteristic in the entire solar spectrum regime as compared with the as-prepared sample. The sudden change in the reflectance spectrum, the extreme increase in emittance and the abrupt change in the surface roughness explain the degradation of the selective performance of the coatings. This performance degradation can be attributed to some microstructural degradation such as reaction between sub-layers leading to phase transformation, phase decomposition/oxidation as observed in case of other absorber coatings [66].

5. Conclusions:

WAlN/WAlON/Al_2O_3-based new solar selective absorber coating on stainless steel substrate was successfully fabricated by DC/RF magnetron sputtering technique. The design was based on the concept of multilayer stack with a pure metallic tungsten layer as an infrared mirror, followed by two absorption layers (WAlN and WAlON) for the maximum absorption of solar energy and an antireflection layer (Al_2O_3) to reduce the reflectance in the solar spectrum. The composition of each layer were tailored to exhibit

maximum spectral selectivity with high solar absorptance of 0.958 and low thermal emittance of 0.08. The absorptance and emittance values of the coating, measured using reflectometer and emissometer, are consistent with the reflectance spectra of UV-Vis-NIR and FTIR spectrophotometer. The thermal stability of the coating established up to a temperature of 500°C in air for 2 hours and this was attributed to high oxidation resistance of individual layers as well as the presence of metallic tungsten layer and Al_2O_3 as a diffusion barrier. Taken together, WAlN/WAlON/Al_2O_3- based tandem absorber coating with desired combination of the spectral properties and high thermal stability represents a new candidate materials for concentrated solar power applications.

Acknowledgments:

The authors acknowledge Dr. P. Bera, Mr. Srinivas, Mr. Praveen Kumar, Mr. Siju, Mrs. Latha for XPS, UV-Vis-NIR, XRD, AFM, SEM and micro-Raman measurements. The authors thank Dr. Girish M. Gouda, LEOS, ISRO Bangalore for the reflectance measurement in the infrared range. This paper is based upon work supported in part under the US-India Partnership to Advance Clean Energy-Research (PACE-R) for the Solar Energy Research Institute for India and the United States (SERIIUS), funded jointly by the U.S. Department of Energy (Office of Science, Office of Basic Energy Sciences, and Energy Efficiency and Renewable Energy, Solar Energy Technology Program, under Subcontract DE-AC36-08GO28308 to the National Renewable Energy Laboratory, Golden, Colorado) and the Government of India, through the Department of Science and Technology under Subcontract IUSSTF/JCERDC-SERIIUS/2012 dated 22nd Nov. 2012 Atasi Dan thanks DST for providing INSPIRE scholarship. Jyothi J acknowledges CSIR for NET fellowship.

References:

[1] H.L. Zhang, J. Baeyens, J. Degrève, G. Cacères, Concentrated solar power plants: Review and design methodology, Renewable and Sustainable Energy Reviews, 22 (2013) 466-481.
[2] D. Barlev, R. Vidu, P. Stroeve, Innovation in concentrated solar power, Solar energy materials and solar cells, 95 (2011) 2703-2725.
[3] A. Ambrosini, T.N. Lambert, M. Bencomo, A. Hall, N.P. Siegel, C.K. Ho, Improved high temperature solar absorbers for use in concentrating solar power central receiver applications, in, American Society of Mechanical Engineers, pp. 587-594.
[4] C.E. Kennedy, Review of mid-to high-temperature solar selective absorber materials, National Renewable Energy Laboratory Golden Colorado, 2002.
[5] B.O. Seraphin, Solar energy conversion: solid-state physics aspects, Solar Energy Conversion: Solid-state Physics Aspects, 1 (1979).
[6] G. McDonald, A preliminary study of a solar selective coating system using a black cobalt oxide for high temperature solar collectors, Thin Solid Films, 72 (1980) 83-88.
[7] T. Maruyama, Copper oxide thin films prepared by chemical vapor deposition from copper dipivaloylmethanate, Solar energy materials and solar cells, 56 (1998) 85-92.
[8] A. Amri, Z.T. Jiang, T. Pryor, C.-Y. Yin, S. Djordjevic, Developments in the synthesis of flat plate solar selective absorber materials via sol–gel methods: A review, Renewable and Sustainable Energy Reviews, 36 (2014) 316-328.
[9] S.W. Moore, Solar absorber selective paint research, Solar energy materials, 12 (1985) 435-447.
[10] N. Selvakumar, H.C. Barshilia, Review of physical vapor deposited (PVD) spectrally selective coatings for mid-and high-temperature solar thermal applications, Solar Energy Materials and Solar Cells, 98 (2012) 1-23.
[11] C. Atkinson, C.L. Sansom, H.J. Almond, C.P. Shaw, Coatings for concentrating solar systems–A review, Renewable and Sustainable Energy Reviews, 45 (2015) 113-122.
[12] C. H Trease, H. Hadavinia, P. E Barrington, Solar Selective Coatings: Industrial State-of-the-Art, Recent Patents on Materials Science, 6 (2013) 1-19.
[13] H.C. Barshilia, Growth, characterization and performance evaluation of Ti/AlTiN/AlTiON/AlTiO high temperature spectrally selective coatings for solar thermal power applications, Solar energy materials and solar cells, 130 (2014) 322-330.
[14] L. Rebouta, A. Pitães, M. Andritschky, P. Capela, M.F. Cerqueira, A. Matilainen, K. Pischow, Optical characterization of TiAlN/TiAlON/SiO_2 absorber for solar selective applications, Surface and Coatings Technology, 211 (2012) 41-44.
[15] Y. Wu, C. Wang, Y. Sun, Y. Ning, Y. Liu, Y. Xue, W. Wang, S. Zhao, E. Tomasella, A. Bousquet, Study on the thermal stability of Al/NbTiSiN/NbTiSiON/SiO_2 solar selective absorbing coating, Solar Energy, 119 (2015) 18-28.
[16] M. Du, X. Liu, L. Hao, X. Wang, J. Mi, L. Jiang, Q. Yu, Microstructure and thermal stability of Al/$Ti_{0.5}Al_{0.5}N$/$Ti_{0.25}Al_{0.75}N$/AlN solar selective coating, Solar energy materials and solar cells, 111 (2013) 49-56.
[17] H. Du, H. Zhao, J. Xiong, G. Xian, Effect of interlayers on the structure and properties of TiAlN based coatings on WC-Co cemented carbide substrate, International Journal of Refractory Metals and Hard Materials, 37 (2013) 60-66.
[18] Y. Liu, C. Wang, Y. Xue, The spectral properties and thermal stability of NbTiON solar selective absorbing coating, Solar energy materials and solar cells, 96 (2012) 131-136.
[19] H.C. Barshilia, N. Selvakumar, K.S. Rajam, D.V.S. Rao, K. Muraleedharan, A. Biswas, TiAlN/TiAlON/Si_3N_4 tandem absorber for high temperature solar selective applications, Applied physics letters, 89 (2006) 191909-191909.
[20] H.C. Barshilia, N. Selvakumar, K.S. Rajam, A. Biswas, Spectrally selective NbAlN/NbAlON/Si_3N_4 tandem absorber for high-temperature solar applications, Solar energy materials and solar cells, 92 (2008) 495-504.

[21] Y. Wu, C. Wang, Y. Sun, Y. Xue, Y. Ning, W. Wang, S. Zhao, E. Tomasella, A. Bousquet, Optical simulation and experimental optimization of Al/NbMoN/NbMoON/SiO_2 solar selective absorbing coatings, Solar energy materials and solar cells, 134 (2015) 373-380.
[22] C. Zou, L. Huang, J. Wang, S. Xue, Effects of antireflection layers on the optical and thermal stability properties of a spectrally selective CrAlN–CrAlON based tandem absorber, Solar energy materials and solar cells, 137 (2015) 243-252.
[23] M. Ishida, I. Katakabe, T. Nakamura, N. Ohtake, Epitaxial Al_2O_3 films on Si by low-pressure chemical vapor deposition, Applied physics letters, 52 (1988) 1326-1328.
[24] Y. Dong, J. Li, Tungsten nitride nanocrystals on nitrogen-doped carbon black as efficient electrocatalysts for oxygen reduction reactions, Chemical Communications, 51 (2015) 572-575.
[25] Y.M. Zhao, W.B. Hu, Y.D. Xia, E.F. Smith, Y.Q. Zhu, C.W. Dunnill, D.H. Gregory, Preparation and characterization of tungsten oxynitride nanowires, Journal of Materials Chemistry, 17 (2007) 4436-4440.
[26] M. Hasheminiasari, J. Lin, The Process Optimization of Smart Nanostructured AlN Thin Films Sputtered by Pulsed DC, JOM, 67 (2015) 867-871.
[27] C. Hinnen, D. Imbert, J.M. Siffre, P. Marcus, An in situ XPS study of sputter-deposited aluminium thin films on graphite, Applied surface science, 78 (1994) 219-231.
[28] L. Colombo, J.J. Chambers, M.R. Visokay, Refractory metal-based electrodes for work function setting in semiconductor devices, in, Google Patents, 2008.
[29] S. Schoser, G. Bräuchle, J. Forget, K. Kohlhof, T. Weber, J. Voigt, B. Rauschenbach, XPS investigation of AlN formation in aluminum alloys using plasma source ion implantation, Surface and Coatings Technology, 103 (1998) 222-226.
[30] L. Rosenberger, R. Baird, E. McCullen, G. Auner, G. Shreve, XPS analysis of aluminum nitride films deposited by plasma source molecular beam epitaxy, Surface and Interface Analysis, 40 (2008) 1254-1261.
[31] D.D. Kumar, N. Kumar, S. Kalaiselvam, S. Dash, R. Jayavel, Substrate effect on wear resistant transition metal nitride hard coatings: Microstructure and tribo-mechanical properties, Ceramics International, (2015).
[32] S. Bao, K.H. Lee, G.Y. Chong, E.A. Fitzgerald, C.S. Tan, AlN-AlN Layer Bonding and Its Thermal Characteristics, ECS Journal of Solid State Science and Technology, 4 (2015) P200-P205.
[33] Y.G. Shen, Y.W. Mai, Effect of deposition conditions on internal stresses and microstructure of reactively sputtered tungsten nitride films, Surface and Coatings Technology, 127 (2000) 238-245.
[34] L. Salvati Jr, L.E. Makovsky, J.M. Stencel, F.R. Brown, D.M. Hercules, Surface spectroscopic study of tungsten-alumina catalysts using X-ray photoelectron, ion scattering, and Raman spectroscopies, The Journal of Physical Chemistry, 85 (1981) 3700-3707.
[35] L.-G. Wang, X. Qian, Y.-Q. Cao, Z.-Y. Cao, G.-Y. Fang, A.-D. Li, D. Wu, Excellent resistive switching properties of atomic layer-deposited $Al_2O_3/HfO_2/Al_2O_3$ trilayer structures for non-volatile memory applications, Nanoscale research letters, 10 (2015) 1-8.
[36] L.J. Saethre, N. Martensson, S. Svensson, P.A. Malmquist, U. Gelius, K. Siegbahn, Gas phase ESCA studies of 2, 5-diaza-1, 6-dioxa-6a-thiapentalene and its selenium and tellurium analogs, Journal of the American Chemical Society, 102 (1980) 1783-1788.
[37] H.L. Zhang, D.Z. Wang, N.K. Huang, The effect of nitrogen ion implantation on tungsten surfaces, Applied surface science, 150 (1999) 34-38.
[38] Z.Y. Nuru, M. Msimanga, T.F.G. Muller, C.J. Arendse, C. Mtshali, M. Maaza, Microstructural, optical properties and thermal stability of MgO/Zr/MgO multilayered selective solar absorber coatings, Solar Energy, 111 (2015) 357-363.
[39] B.O. Seraphin, Spectrally selective surfaces and their impact on photothermal solar energy conversion, Springer, 1979.
[40] E. Valova, J. Georgieva, S. Armyanov, S. Sotiropoulos, A. Hubin, K. Baert, M. Raes, Morphology, structure and photoelectrocatalytic activity of TiO_2/WO_3 coatings obtained by

pulsed electrodeposition onto stainless steel, Journal of the Electrochemical Society, 157 (2010) D309-D315.
[41] Y.F. Lu, H. Qiu, Laser coloration and bleaching of amorphous WO_3 thin film, Journal of Applied Physics, 88 (2000) 1082-1087.
[42] J. Diaz-Reyes, J.E. Flores-Mena, J.M. Gutierrez-Arias, M.M. Morin-Castillo, H. Azucena-Coyotecatl, M. Galvan, P. Rodriguez-Fragoso, A. Mendez-Lopez, Optical and structural properties of WO_3 as a function of the annealing temperature, in, World Scientific and Engineering Academy and Society (WSEAS), pp. 99-104.
[43] L. Wang, X. Lu, C. Han, R. Lu, S. Yang, X. Song, Electrospun hollow cage-like α-Fe_2O_3 microspheres: synthesis, formation mechanism, and morphology-preserved conversion to Fe nanostructures, CrystEngComm, 16 (2014) 10618-10623.
[44] S. Dass, R. Shrivastav, V.R. Satsangi, Enhanced photoelectrochemical hydrogen production with swift heavy ion irradiation.
[45] A. Dan, K. Chattopadhyay, H.C. Barshilia, B. Basu, Angular solar absorptance and thermal stability of W/WAlN/WAlON/Al_2O_3-based solar selective absorber coating, Applied Thermal Engineering, (2016).
[46] A. Dan, K. Chattopadhyay, H.C. Barshilia, B. Basu, Thermal stability of WAlN/WAlON/Al_2O_3 -based solar selective absorber coating, MRS Advances, CJO2016. (2016) doi:10.1557/adv.2016.1388.
[47] A. Soum-Glaude, I. Bousquet, L. Thomas, G. Flamant, Optical modeling of multilayered coatings based on SiC (N) H materials for their potential use as high-temperature solar selective absorbers, Solar energy materials and solar cells, 117 (2013) 315-323.
[48] L. Wu, J. Gao, Z. Liu, L. Liang, F. Xia, H. Cao, Thermal aging characteristics of CrN_xO_y solar selective absorber coating for flat plate solar thermal collector applications, Solar energy materials and solar cells, 114 (2013) 186-191.
[49] K.P. Sibin, S. John, H.C. Barshilia, Control of thermal emittance of stainless steel using sputtered tungsten thin films for solar thermal power applications, Solar energy materials and solar cells, 133 (2015) 1-7.
[50] N. Selvakumar, K. Rajaguru, G.M. Gouda, H.C. Barshilia, AlMoN based spectrally selective coating with improved thermal stability for high temperature solar thermal applications, Solar Energy, 119 (2015) 114-121.
[51] Y. Xue, C. Wang, Y. Sun, Y. Wu, Y. Ning, W. Wang, Effects of the LMVF and HMVF absorption layer thickness and metal volume fraction on optical properties of the $MoSi_2$–Al_2O_3 solar selective absorbing coating, Vacuum, 104 (2014) 116-121.
[52] V. Teixeira, E. Sousa, M.F. Costa, C. Nunes, L. Rosa, M.J. Carvalho, M. Collares-Pereira, E. Roman, J. Gago, Spectrally selective composite coatings of Cr–Cr_2O_3 and Mo–Al_2O_3 for solar energy applications, Thin Solid Films, 392 (2001) 320-326.
[53] M. Farooq, Z.H. Lee, Computations of the optical properties of metal/insulator-composites for solar selective absorbers, Renewable energy, 28 (2003) 1421-1431.
[54] C. Nunes, V. Teixeira, M.L. Prates, N.P. Barradas, A.D. Sequeira, Graded selective coatings based on chromium and titanium oxynitride, Thin Solid Films, 442 (2003) 173-178.
[55] S. Zhao, E. Wäckelgård, The optical properties of sputtered composite of Al–AlN, Solar energy materials and solar cells, 90 (2006) 1861-1874.
[56] A. Soum-Glaude, I. Bousquet, M. Bichotte, S. Quoizola, L. Thomas, G. Flamant, Optical Characterization and Modeling of Coatings Intended as High Temperature Solar Selective Absorbers, Energy Procedia, 49 (2014) 530-537.
[57] L. Rebouta, P. Capela, M. Andritschky, A. Matilainen, P. Santilli, K. Pischow, E. Alves, Characterization of TiAlSiN/TiAlSiON/SiO_2 optical stack designed by modelling calculations for solar selective applications, Solar energy materials and solar cells, 105 (2012) 202-207.

[58] H.C. Barshilia, N. Selvakumar, K.S. Rajam, A. Biswas, Optical properties and thermal stability of TiAlN/AlON tandem absorber prepared by reactive DC/RF magnetron sputtering, Solar energy materials and solar cells, 92 (2008) 1425-1433.
[59] Q.-C. Zhang, Optimizing analysis of W-AlN cermet solar absorbing coatings, Journal of Physics D: Applied Physics, 34 (2001) 3113.
[60] S. Zhao, E. Avendaño, K. Gelin, J. Lu, E. Wäckelgård, Optimization of an industrial DC magnetron sputtering process for graded composition solar thermal absorbing layer, Solar energy materials and solar cells, 90 (2006) 308-328.
[61] Q.-C. Zhang, Recent progress in high-temperature solar selective coatings, Solar energy materials and solar cells, 62 (2000) 63-74.
[62] S. Zhao, E. Wäckelgård, Optimization of solar absorbing three-layer coatings, Solar energy materials and solar cells, 90 (2006) 243-261.
[63] T. Boström, E. Wäckelgård, G. Westin, Solution-chemical derived nickel–alumina coatings for thermal solar absorbers, Solar Energy, 74 (2003) 497-503.
[64] A. Soum-Glaude, I. Bousquet, L. Thomas, G. Flamant, Optical modeling of multilayered coatings based on SiC(N)H materials for their potential use as high-temperature solar selective absorbers, Solar energy materials and solar cells, 117 (2013) 315-323.
[65] R.E. Peterson, J.W. Ramsey, Thin film coatings in solar− thermal power systems, Journal of Vacuum Science & Technology, 12 (1975) 174-181.
[66] J. Jyothi, H. Chaliyawala, G. Srinivas, H.S. Nagaraja, H.C. Barshilia, Design and fabrication of spectrally selective TiAlC/TiAlCN/TiAlSiCN/TiAlSiCO/TiAlSiO tandem absorber for high-temperature solar thermal power applications, Solar energy materials and solar cells, 140 (2015) 209-216.

Table 1

Processing parameters of the optimized WAlN/WAlON/Al_2O_3 coating

Layer	**Gas flow rate (sccm)**			**Deposition time (min)**	**W target power density (W/cm^2)**	**Al target power density (W/cm^2)**	**Al_2O_3 target power density (W/cm^2)**	**Test temperature (°C)**
	Ar	**O_2**	**N_2**					
W	28	-	-	15	3.114	0.340	-	300
WAlN	28	-	26	6	1.698	2.265	-	300
WAlON	28	9	21	6	1.982	2.548	-	300
Al_2O_3	20	2	-	6.5	-	-	6.582	RT

Table 2

Variation of absorptance and emittance with deposition time

Layer	Ar (sccm)	O_2 (sccm)	N_2 (sccm)	Deposition time (min)	Absorptance (α)	Emittance (ε)
WAlN	28	-	26	5.5	0.730	0.08
	28	-	26	**6**	**0.753**	0.08
	28	-	26	8	0.732	0.08
WAlON	28	9	21	5	0.871	0.08
	28	9	21	**6**	**0.902**	0.08
	28	9	21	7	0.882	0.08
Al_2O_3	20	-	2	6	0.944	0.08
	20	-	2	**6.5**	**0.958**	0.08
	20	-	2	8	0.924	0.08

Table 3

Summary of XPS analysis of WAlN, WAlON and Al_2O_3 layers

Layer	Elements	Peak	Binding energy (eV)	Electronic Transition	Chemical bonding	Reference
WAlN	W	1	32.7	$4f_{7/2}$	W-N	[24]
		2	34.7	$4f_{5/2}$	W-N	[24]
		3	36.2	$4f_{7/2}$	W-O	[25]
		4	38.4	$4f_{5/2}$	W-O	[25]
	Al	1	72.9	2p	Metallic Al	[26]
		2	73.5		Al-N	[27]
		3	74.5		Al-O	[28]
		4	75.2		Al-O-N	[29]
	N	1	396.3	1s	N-Al	[30]
		2	396.7		N-W	[31]
		3	397.7		N-W	[31]
		4	398.6		N-Al-O	[32]
		5	400.1		Interstitial site of W_2N	[33]
	O	1	530.5	1s	O-W	[34]
		2	531.5		O-Al	[35]
		3	532.8		Chemisorption of water	[36]
		4	532.9		O_X-W	[37]
WAlON	W	1	36.6	$4f_{7/2}$	W-O	[25]
		2	38.7	$4f_{5/2}$	W-O	[25]
	Al	1	75.3	2p	Al-O-N	[29]
	O	1	530.5	1s	O-W	[34]
		2	531.6		O-Al	[35]
		3	532.8		Chemisorption of water	[36]
		4	532.9		Ox-W	[37]
	N	1	396.7	1s	N-W	[31]
		2	397.7		N-W	[31]

		3	400.7		N-W	[33]
Al_2O_3	Al	1	72.9	2p	Metallic Al	[26]
		2	73.5		Al-N	[27]
		3	74.5		Al-O	[28]
		4	75.2		Al-O-N	[29]
	O	1	530.5	1s	O-W	[34]
		2	531.6		O-Al	[35]
		3	532.7		Chemisorption of water	[36]
		4	532.9		O_X-W	[37]

Table 4

Absorptance and emittance of SS substrate and different layers of the solar selective coating

Layers	**Absorptance (α)**	**Emittance (ε)**	**Selectivity (α/ε)**
SS	0.387-0.380	0.12-0.13	3.22
W	0.500	0.08	6.25
W/WAlN	0.753	0.08	9.41
W/WAlN/ WAlON	0.902	0.08	11.27
W/WAlN/WAlON/Al_2O_3	0.958	0.08	11.97

List of Figures:

Figure 1

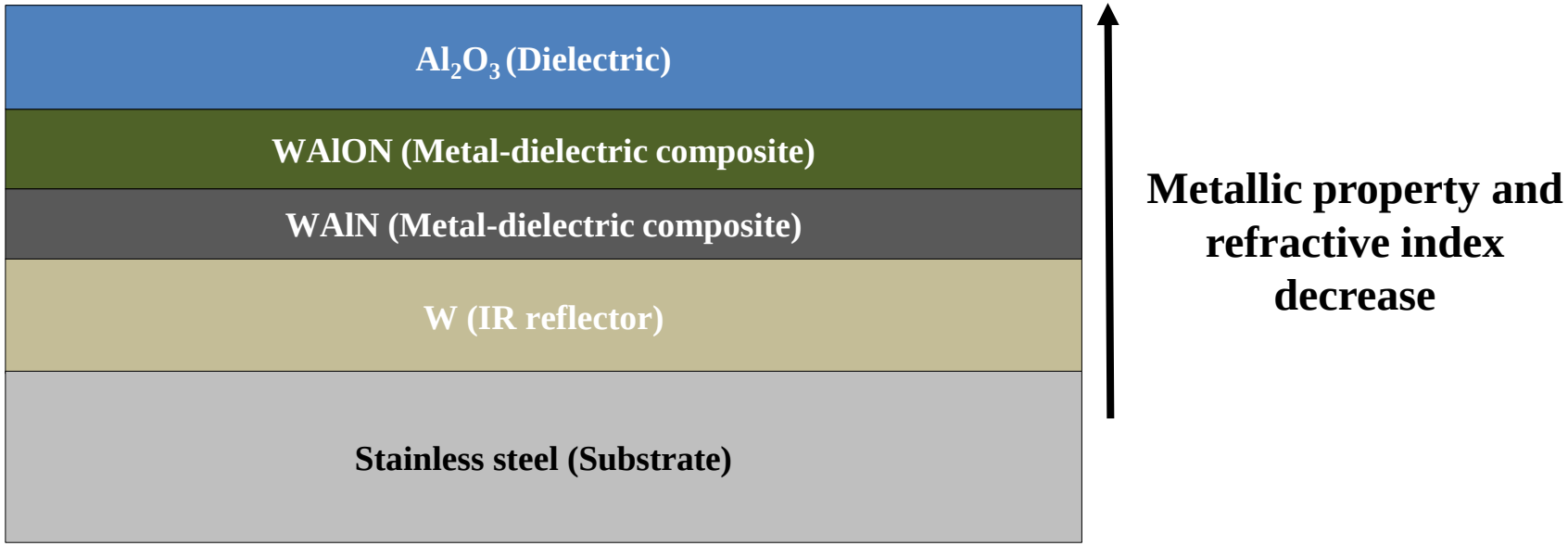

Fig. 1. Schematic diagram of the W/WAlN/WAlON/Al_2O_3 tandem absorber. Graded metallic profile has been designed [61-63]

Figure 2

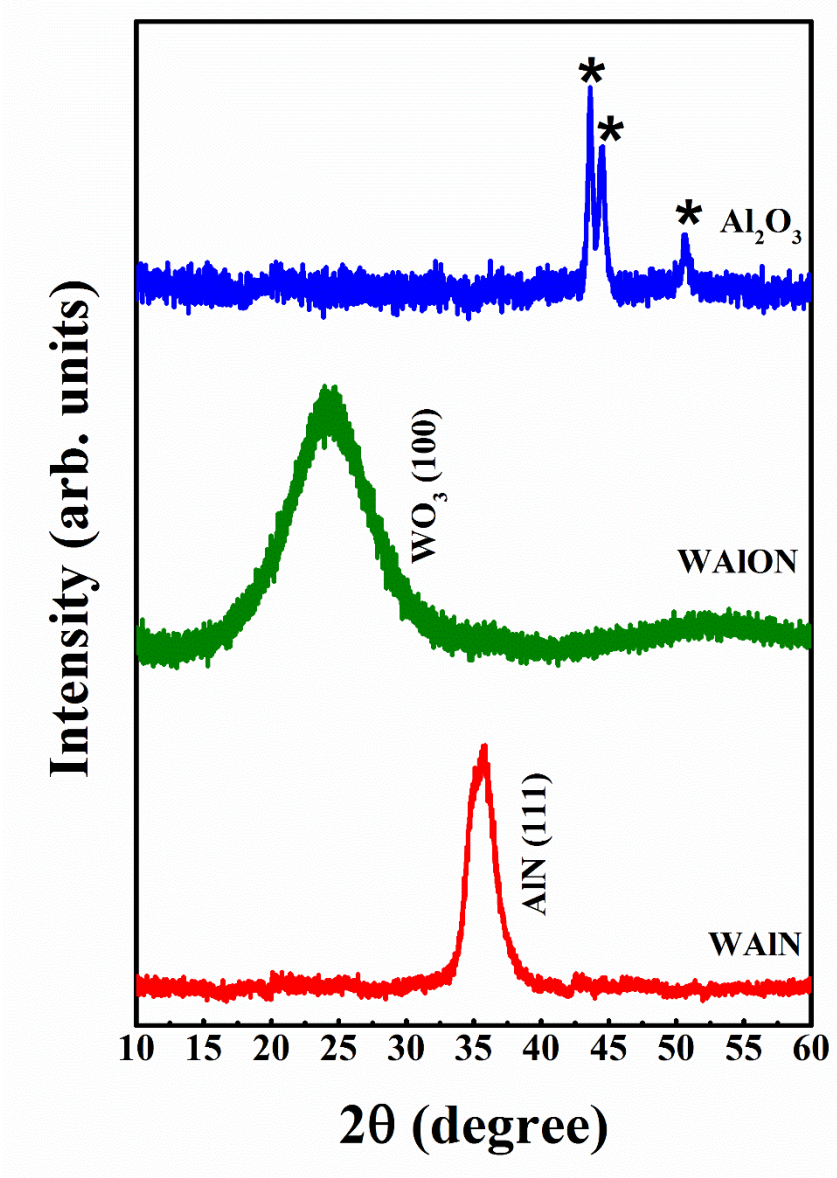

Fig. 2. XRD patterns of WAlN, WAlON and Al_2O_3 coating deposited for longer duration on stainless steel substrate

Figure 3

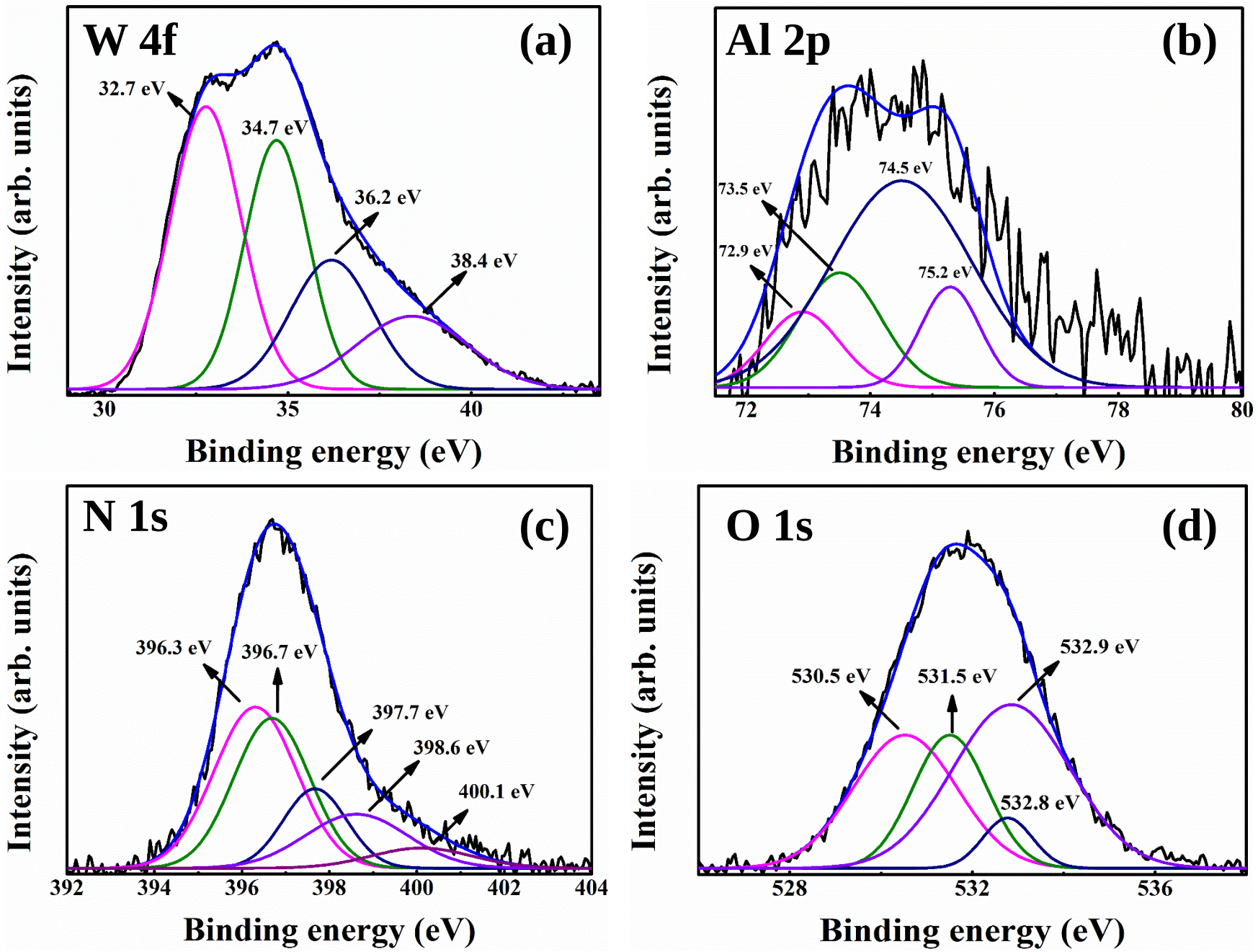

Fig. 3. XPS spectra of WAlN coating (a) W 4f (b) Al 2p (c) N 1s and (d) O 1s

Figure 4

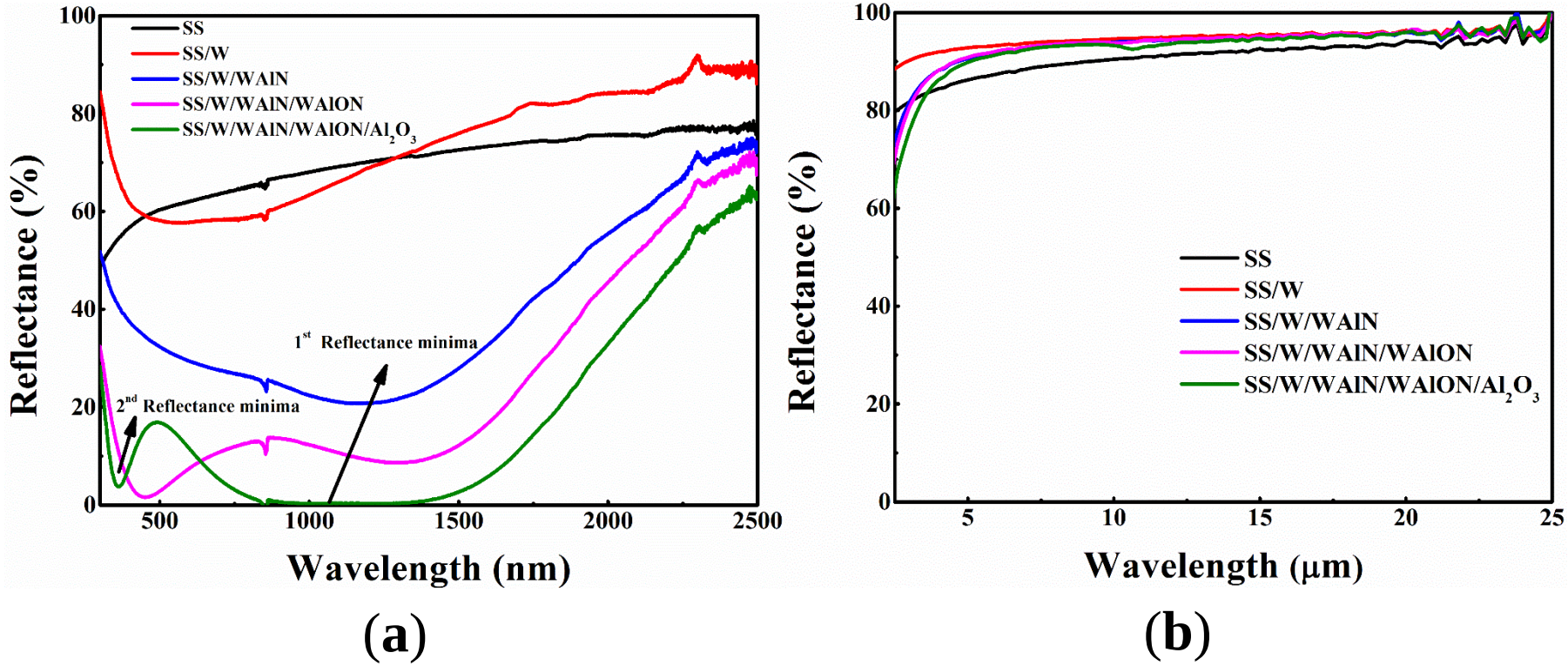

Fig. 4. Reflectance spectra of (a) layer- added tandem absorber in solar spectrum range; (b) Infra-red range deposited on stainless steel substrate

Figure 5

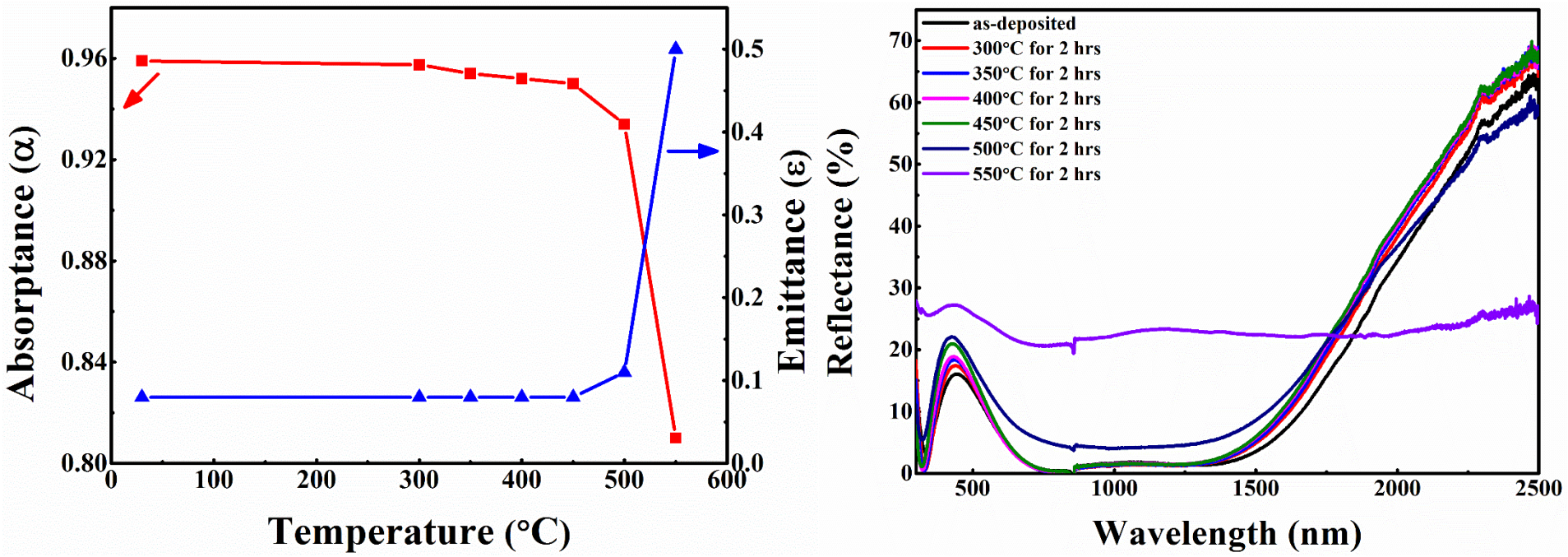

Fig. 5. (a) Temperature dependence of solar absorptance and emittance; (b) Reflectance spectra of as-deposited and heat treated coating in air for 2hrs

Figure 6

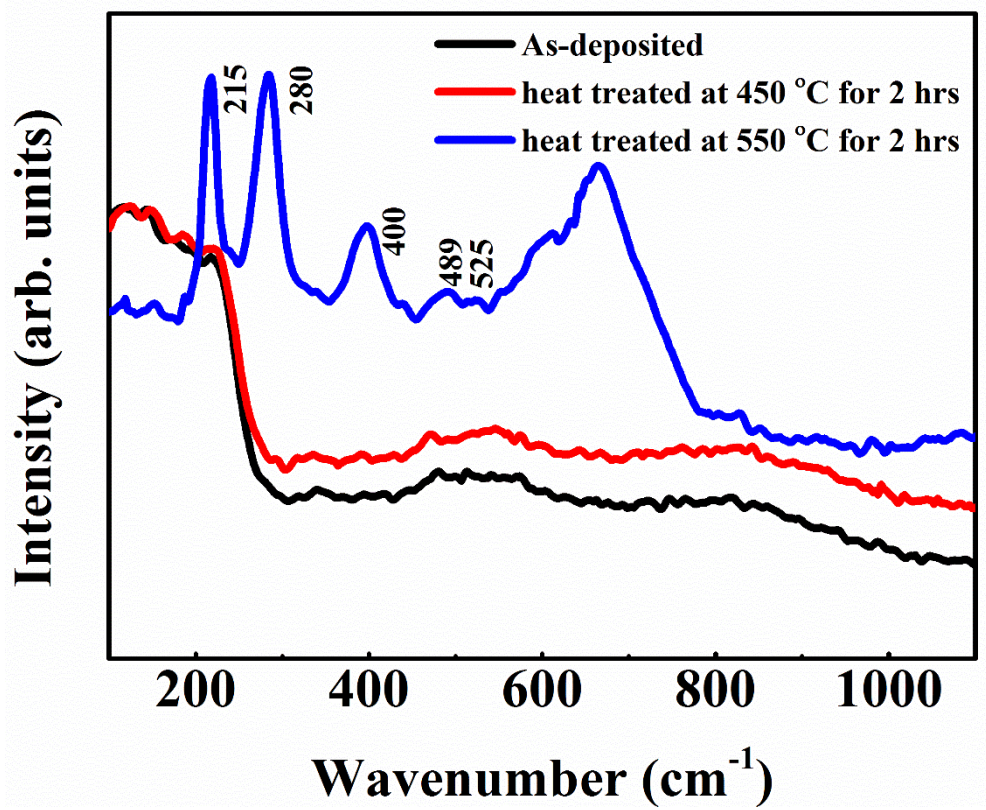

Fig. 6. Raman spectrum of as-deposited and heat treated coating at 450 and 550 °C for 2 hrs in air

Figure 7

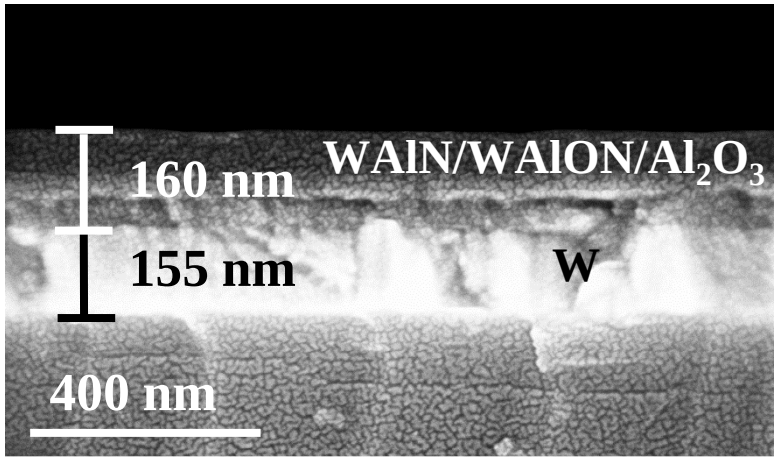

Fig. 7. Cross sectional FESEM image of multi-layer coating

Figure 8

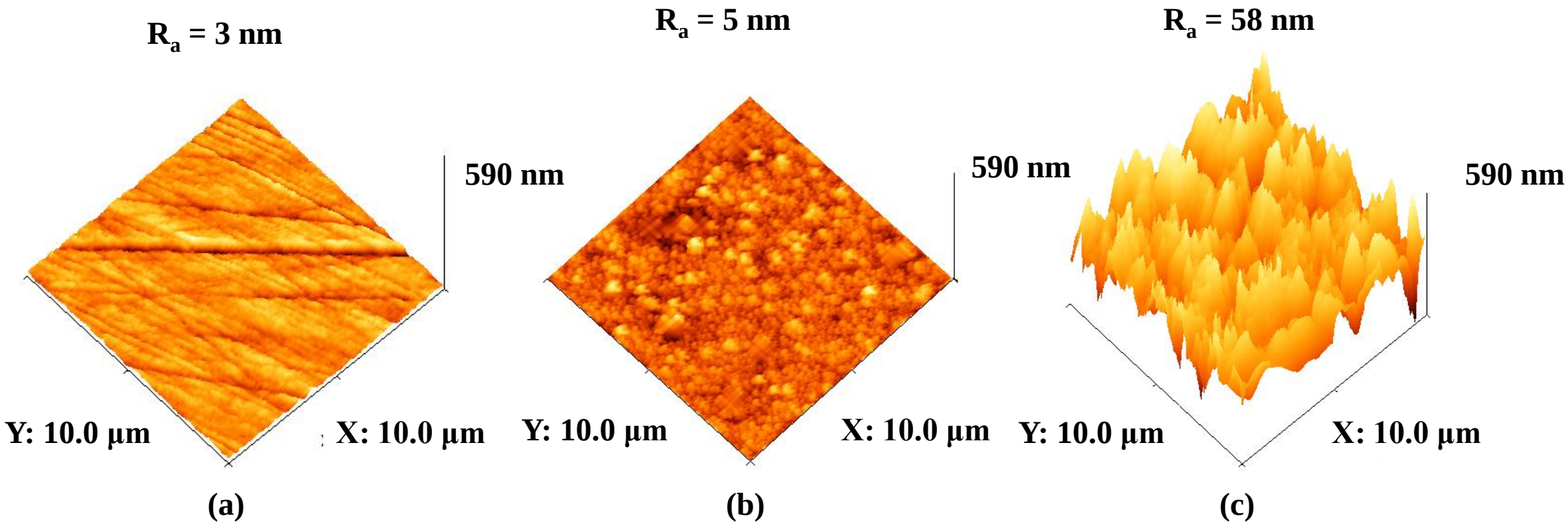

Fig. 8. 3D AFM image of (a) as-deposited coating; (b) heat treated coating at 450 °C ; and (c) 550 °C